

Compact stars with color superconducting quark matter

Mark Alford^(a), Sanjay Reddy^{(b),(c)}

^(a) Physics and Astronomy Department,
Glasgow University,
Glasgow G12 8QQ, U.K.

^(b) Center for Theoretical Physics,
Massachusetts Institute of Technology,
Cambridge, MA 02139, U.S.A.

^(c) Theoretical Division,
Los Alamos National Laboratory,
Los Alamos, NM 87545, U.S.A.

Nov 14, 2002

GUTPA/02/11/01

Abstract

We study compact stars that contain quark matter. We look at the effect of color superconductivity in the quark matter on the nuclear-quark matter transition density, mass-radius relationship, and the density discontinuity at the boundary between nuclear and quark matter. We find that color superconducting quark matter will occur in compact stars at values of the bag constant where ordinary quark matter would not be allowed. We are able to construct “hybrid” stars with a color superconducting quark matter interior and nuclear matter surface, with masses in the range 1.3-1.6 M_{\odot} and radii 8-11 km. Our results are consistent with recent mass-radius limits based on absorption lines from EXO0748-676.

1 Introduction

If matter is compressed far enough beyond nuclear density then there is a transition from nuclear matter to quark matter. It is becoming widely accepted that quark matter will typically be in a color-superconducting phase [1, 2, 3, 4, 5], in which the quarks near the Fermi surface form Cooper pairs which condense, breaking the color gauge symmetry (for reviews see Ref. [6]). The pairing pattern favored at sufficiently high density is the color-flavor locked (CFL) phase in which up-down, down-strange, and up-strange Cooper pairs all form, allowing quarks of all three colors and all three flavors to pair [5].

One of the most likely locations for quark matter in nature is the interior of compact stars, where pressure due to gravity drives the density above nuclear density, and the temperature is low compared with nuclear/quark energy scales. Various possible signatures of color superconductivity in compact stars have been studied, mostly focusing on transport properties (for a recent review, see Ref. [7]). Although the effect of unpaired quark matter on the compact star mass-radius relationship is an active area of research [8, 9, 10], the consequences of color superconducting quark matter have not yet been investigated.

The contribution of color superconductivity with gap Δ to the pressure p of quark matter is of order $\mu^2\Delta^2$, which is dominated by the leading order μ^4 contribution from the Fermi sea. However, quark matter must also pay a free-energy cost, the bag constant B , relative to the confined vacuum:

$$p \sim \mu^4 + \Delta^2\mu^2 - B. \quad (1.1)$$

If the bag constant is large enough so that nuclear matter and quark matter have comparable pressures at some density that occurs in compact stars, then the superconducting gap Δ may have a large effect on the equation of state and hence on the mass-radius relationship of a compact star. A similar observation has been used recently to show that the region of model space where strange quark matter is absolutely stability is influenced by superconductivity [11].

In this paper we study the gross structure of compact stars, taking into account the possibility of a CFL quark-paired phase of quark matter, as well as unpaired quark matter (UQM). We treat the quark matter as a Fermi sea of free quarks with an additional contribution to the pressure from the formation of the CFL condensate. We treat the nuclear matter as consisting only of protons, neutrons, and electrons, and either obtain the nuclear equation of state from the Walecka model of nuclear interactions, or use the APR98 equation of state [12].

In order to find the effects of color superconductivity, we allow all the phases to compete with each other, selecting the highest pressure phase at each value of the quark chemical potential. If local electrical neutrality is imposed, this leads to sharp interfaces between the different phases. If a globally neutral inter-penetration of two charged phases is allowed, this leads to mixed phases. We study both possibilities. We survey the parameter space of the quark matter, covering a range of values of

the bag constant B , the strange quark mass m_s , and the color superconducting gap Δ . In section 2 we explain our calculation of the equations of state for nuclear and quark matter. In section 3 we obtain the resultant mass-radius relationships, paying particular attention to the maximum masses that can be obtained. Section 4 presents our conclusions.

2 Equations of state

For nuclear matter we use the Walecka equation of state, which allows us to calculate the pressure for any quark chemical potential μ and electron chemical potential μ_e , and hence to construct mixed phases. In section 3.3 we will show results for the APR98 equation of state, which is obtained using non-relativistic variational methods starting from a Hamiltonian that reproduces known nucleon-nucleon scattering data. For nuclear matter at very low densities we use the tabulated Negele-Vautherin [13] and Baym-Pethick-Sutherland [14] equations of state.

2.1 Walecka equation of state

We use the Walecka model as described in [15] and calibrated in [16]. The free energy is

$$\begin{aligned} \Omega_{\text{nuclear}}(\mu_n, \mu_e) = & \frac{1}{\pi^2} \left(\int_0^{k_{Fn}} dk k^2 (\varepsilon_n(k) - \mu_n) + \int_0^{k_{Fp}} dk k^2 (\varepsilon_p(k) - \mu_p) \right) \\ & + \frac{1}{2} (m_\sigma^2 \sigma^2 - m_\omega^2 \omega^2 - m_\rho^2 \rho^2) + U(\sigma) - \frac{\mu_e^4}{12\pi^2}, \end{aligned} \quad (2.1)$$

where

$$\varepsilon_n(k) = \sqrt{k^2 + m_N^{*2}} + g_{\omega N} \omega - \frac{1}{2} g_{\rho N} \rho, \quad (2.2)$$

$$\varepsilon_p(k) = \sqrt{k^2 + m_N^{*2}} + g_{\omega N} \omega + \frac{1}{2} g_{\rho N} \rho, \quad (2.3)$$

are the neutron and proton single particle energies in the mean field approximation. The corresponding Fermi momenta k_{Fn} and k_{Fp} , which minimize the free energy at fixed baryon and electron chemical potentials, are given by solving

$$\begin{aligned} \varepsilon_n(k_{Fn}) &= \mu_n, \\ \varepsilon_p(k_{Fp}) &= \mu_p, \end{aligned} \quad (2.4)$$

where weak equilibrium sets $\mu_p = \mu_n - \mu_e$, and

$$\begin{aligned} m_\sigma^2 \sigma &= g_{\sigma N} (n_s(k_{Fn}) + n_s(k_{Fp})) - \frac{dU}{d\sigma}, \\ m_\omega^2 \omega &= g_{\omega N} (n(k_{Fn}) + n(k_{Fp})), \\ m_\rho^2 \rho &= \frac{1}{2} g_\rho (n(k_{Fp}) - n(k_{Fn})). \end{aligned} \quad (2.5)$$

The nucleon number density n and scalar density n_s for nucleons with Fermi momentum k_F are

$$\begin{aligned} n(k_F) &= \frac{1}{\pi^2} \int_0^{k_F} dk k^2 = \frac{k_F^3}{3\pi^2}, \\ n_s(k_F) &= \frac{1}{\pi^2} \int_0^{k_F} dk k^2 \frac{m_N^*}{\sqrt{k^2 + m_N^{*2}}}, \end{aligned} \quad (2.6)$$

where

$$m_N^* = m_N - g_{\sigma N} \sigma \quad (2.7)$$

is the nucleon effective mass, which is reduced compared to the free nucleon mass m_N due to the scalar field σ , taken to have $m_\sigma = 600$ MeV. The scalar self-interaction term is

$$U(\sigma) = \frac{b}{3} m_N (g_{\sigma N} \sigma)^3 + \frac{c}{4} (g_{\sigma N} \sigma)^4, \quad (2.8)$$

where b and c are dimensionless coupling constants. The five coupling constants, $g_{\sigma N}$, $g_{\omega N}$, $g_{\rho N}$, b , and c , are chosen as in Ref. [16] to reproduce five empirical properties of nuclear matter at saturation density: the saturation density itself is $n_0 = 0.16 \text{ fm}^{-3}$; the binding energy per nucleon is 16 MeV; the nuclear compression modulus is 240 MeV; the nucleon effective mass at saturation density is $0.78 m_N$; and the symmetry energy is 32.5 MeV.

The charge density in nuclear matter is

$$Q_{\text{nuclear}} = \frac{\partial \Omega_{\text{nuclear}}}{\partial \mu_e} \quad (2.9)$$

which is just the number density of protons minus that of electrons. In bulk matter one requires $Q_{\text{nuclear}} = 0$, but not in mixed phases (Section 2.5).

2.2 Unpaired quark matter (UQM) equation of state

In noninteracting unpaired quark matter, the free energy is

$$\begin{aligned} \Omega_{\text{UQM}}(\mu, \mu_e) &= \frac{3}{\pi^2} \int_0^{\nu_u} p^2 (p - \mu) dp + \frac{3}{\pi^2} \int_0^{\nu_d} p^2 (p - \mu) dp \\ &+ \frac{3}{\pi^2} \int_0^{\nu_s} p^2 \left(\sqrt{p^2 + m_s^2} - \mu \right) dp, \end{aligned} \quad (2.10)$$

where the Fermi momenta are

$$\begin{aligned} \nu_u^2 &= (\mu - \frac{2}{3}\mu_e)^2 - m_u^2, \\ \nu_d^2 &= (\mu + \frac{1}{3}\mu_e)^2 - m_d^2, \\ \nu_s^2 &= (\mu + \frac{1}{3}\mu_e)^2 - m_s^2. \end{aligned} \quad (2.11)$$

Differentiating with respect to μ_e , we obtain the charge density

$$Q_{\text{UQM}} = \frac{2}{\pi^2} \frac{\mu^2 \mu_e}{\mu} - \frac{2}{3\pi^2} \mu (\mu_e^2 + \frac{3}{4} m_s^2) - \frac{m_s^2 \mu_e}{6\pi^2} + O \left[\frac{m_s^4}{\mu}, \frac{m_s^4 \mu_e}{\mu^2} \right]. \quad (2.12)$$

2.3 CFL quark matter equation of state

We describe the CFL phase using the free energy

$$\Omega_{\text{CFL}}(\mu, \mu_e) = \Omega_{\text{CFL}}^{\text{quarks}}(\mu) + \Omega_{\text{CFL}}^{\text{GB}}(\mu, \mu_e) + \Omega^{\text{electrons}}(\mu_e) \quad (2.13)$$

The contribution to (2.13) from the quarks is [6, 17]

$$\Omega_{\text{CFL}}^{\text{quarks}} = \frac{6}{\pi^2} \int_0^\nu p^2(p - \mu) dp + \frac{3}{\pi^2} \int_0^\nu p^2 \left(\sqrt{p^2 + m_s^2} - \mu \right) dp - \frac{3\Delta^2 \mu^2}{\pi^2} + B, \quad (2.14)$$

where the quark number densities are $n_u = n_d = n_s = (\nu^3 + 2\Delta^2 \mu)/\pi^2$ and the common Fermi momentum is

$$\nu = 2\mu - \sqrt{\mu^2 + \frac{m_s^2}{3}} \quad (2.15)$$

The first two terms give the free energy of the noninteracting quarks, while the third term is the lowest order (in powers of Δ/μ) contribution from the formation of the CFL condensate.

The contribution to (2.13) from the Goldstone bosons arising due to breaking of chiral symmetry in the CFL phase is denoted $\Omega_{\text{CFL}}^{\text{GB}}(\mu, \mu_e)$. The effective theory describing the octet of mesons has been studied extensively in earlier works [18]. The bulk CFL phase is electrically neutral with the electron chemical potential $\mu_e = 0$ [17]. However, as we shall see in section 2.5, CFL matter in the mixed phase, where $\mu_e > 0$, is electrically charged. When the electron chemical potential exceeds the mass of the lightest negatively charged meson, which in the CFL phase is the π^- , these mesons condense [19, 20]. The free energy in this case is given by

$$\Omega_{\text{CFL}}^{\text{GB}}(\mu) = -\frac{1}{2} f_\pi^2 \mu_e^2 \left(1 - \frac{m_\pi^2}{\mu_e^2} \right)^2, \quad (2.16)$$

where the parameters are [18]

$$f_\pi^2 = \frac{(21 - 8 \log(2)) \mu^2}{36\pi^2}, \quad m_{\pi^-}^2 = \frac{3\Delta^2}{\pi^2 f_\pi^2} m_s (m_u + m_d) .. \quad (2.17)$$

Finally, the contribution to (2.13) from electrons is

$$\Omega^{\text{electrons}}(\mu_e) = -\frac{\mu_e^4}{12\pi^2}. \quad (2.18)$$

Unlike the UQM phase, quark excitations in the CFL phase are gapped, and the lightest charged excitations correspond to pions and kaons. The charge susceptibility in this phase is determined by the effective theory for these collective modes. The

electric charge density (carried by the pion condensate) induced by a electron chemical particle is given by [20]

$$Q_{\text{CFL}} = -f_{\pi}^2 \mu_e \left[1 - \frac{m_{\pi}^4}{\mu_e^4} \right]. \quad (2.19)$$

Meson condensation can occur in the CFL phase even in the absence of an electric charge chemical potential. Bedaque and Schaefer have shown that the strange quark mass introduces a stress on the CFL state and that might result in the condensation of K^0 mesons [19]. Condensation occurs when $m_s^2/2\mu \geq m_{K^0}$, where m_{K^0} is the mass of the K^0 meson in the CFL phase. The free energy due to K^0 -condensed phase is

$$\Omega_{\text{CFL}}^{\text{GB}}(\mu) = -\frac{1}{2} f_{\pi}^2 \frac{m_s^4}{4\mu^2} \left(1 - \frac{4\mu^2 m_{K^0}^2}{m_s^4} \right)^2, \quad (2.20)$$

where the kaon mass [18]

$$m_{K^0}^2 = \frac{3\Delta^2}{\pi^2 f_K^2} m_u (m_d + m_s) .. \quad (2.21)$$

From Eq. (2.20) we see that the free energy due to K^0 -condensation is an order m_s^4 effect and thereby small compared to the $\Delta^2 \mu^2$ contribution to the free energy for $\Delta \sim 100$ MeV. For this reason we neglect K^0 condensation in this study.

2.4 Is color superconductivity important for bulk structure?

We see from (2.14) that color superconductivity contributes $\mathcal{O}(\mu^2 \Delta^2)$ to the free energy, which is small relative to the kinetic energy density which is $\mathcal{O}(\mu^4)$. This well known suppression is a consequence of the fact that pairing is a Fermi surface phenomena and the superconducting gap is usually small compared to the chemical potential. Naively, this would lead us to conclude to that superconductivity will not greatly affect the equation of state of quark matter. If this were true, we should expect that the mass radius relation of neutron stars containing superconducting quark matter would be nearly identical to those constructed in earlier works wherein the role of superconductivity was neglected. However, the truth is more complicated. In the bag model description of quark matter, the free energy gets an additional contribution due to the bag constant. The kinetic pressure and bag pressure cancel when the quark chemical potential

$$\mu_0 = \left(\frac{4\pi^2 B}{3} \right)^{\frac{1}{4}} + O\left(\frac{m_s^2}{\mu} \right). \quad (2.22)$$

Thus, for a given B , there is a narrow window in quark chemical potential in which the pairing contribution to the pressure is dominant. In the vicinity of μ_0 , superconductivity will therefore make a significant contribution to the equation of

Bag constant		CFL	chemical	transition	nuclear	CFL
$B^{1/4}$	B	gap	potential	pressure	density	density
(MeV)	(MeV/fm ³)	(MeV)	(MeV)	(MeV/fm ³)	(n_{sat})	(n_{sat})
190	169.6	0	422.5	111.5	3.464	5.833
190	169.6	50	408.2	88.68	3.158	5.405
190	169.6	100	365.4	33.79	2.149	4.295
170	108.7	0	352.6	21.62	1.805	3.297
170	108.7	50	338.4	10.77	1.382	3.033

Table 1: Properties of the nuclear-quark phase transition for various bag constants B and color-superconducting gaps. Nuclear matter is treated using the Walecka model. The size of the gap has a significant effect on the pressure at which the phase transition occurs and the densities of the two phases there.

state of quark matter. For $B^{1/4}$ in the range 150-200 MeV ($B = 66$ -210 MeV/fm³), we find $\mu_0 \simeq 320 - 400$ MeV. This is an interesting range of chemical potentials because the phase transition from nuclear matter to quark matter typically occurs here. Further, and perhaps more importantly, the pairing contribution to the pressure of CFL quark matter, $P_\Delta = 3\Delta^2\mu^2/\pi^2$, can be comparable or larger than the pressure in the nuclear phase at the same baryon chemical potential. Superconductivity will thereby significantly influence the critical chemical potential at which the transition from nuclear to quark matter occurs. This is clear from Fig. 1, where the transition from NM to QM occurs at a much lower pressure for CFL QM ($a \rightarrow b$) than for unpaired QM ($c \rightarrow d$). The critical chemical potential for the transition for different values of the bag constant and the superconducting gap are shown in table 1.

2.5 Mixed phases

In the preceding discussion we have enforced local charge neutrality in the nuclear and quark phases. We have neglected the possibility of having a mixed phase containing positively charged nuclear matter co-existing with negatively charged CFL matter[21]. Such a possibility was considered in Ref. [22] where the bulk free energy difference between the homogeneous phases and the heterogeneous mixed phase was calculated. The free energy difference between the homogeneous phase and the mixed phase was found to be quite small. If one accounted for the additional surface energy cost in the mixed phase, it was found that even modest values of the surface tension, $\sigma_{\text{NM-CFL}} \sim 30$ MeV were sufficient to disfavor the mixed phase. Nonetheless, we consider this possibility in this work for two reasons. First, the surface tension between the nuclear matter and CFL matter is poorly known. Second, in the case of unpaired quark matter, allowing for a mixed phase has been shown to significantly affect the equation of state over a wide range of pressures and consequently modify the mass-radius relation. This indicates that the

superconducting case warrants investigation.

The procedure to construct the mixed phase between nuclear matter and CFL matter was outlined in Ref. [22]. We follow the same prescription here but briefly note some salient features which distinguish the nuclear-CFL mixed phase from the mixed phase between nuclear matter and unpaired quark matter. The volume fraction of the nuclear and quark phases in the mixed phase is determined by the requirement of global charge neutrality. Denoting the charge density of the nuclear phase by Q_{nuclear} and the charge density of the CFL phase as Q_{CFL} , the volume fraction of the CFL phase is

$$\chi = \frac{V_{\text{CFL}}}{V} = \frac{Q_{\text{nuclear}}}{Q_{\text{nuclear}} - Q_{\text{CFL}}} . \quad (2.23)$$

The energy density of the mixed phase is the volume-weighted average of the individual energy densities and is given by $\epsilon = \chi\epsilon_{\text{nuclear}} + (1 - \chi)\epsilon_{\text{CFL}}$. From Eq. (2.23), we see that, if at fixed electron chemical potential the negative charge density of the quark phase is large its volume fraction will be correspondingly smaller. This is important because the charge susceptibilities of the normal and superconducting phases are quite distinct. In the normal phase it is easy to furnish electric charge since there is no gap in the spectrum for quarks. The electric charge densities of the nuclear matter (Walecka), unpaired quark matter, and CFL quark matter phases are given in Eqs. (2.9), (2.12), (2.19).

For typical quark and electron chemical potentials encountered in the neutron star context one finds that the charge density in the normal phase is significantly larger. For example, when $\mu = 400$ MeV, $\mu_e = 100$ MeV and $m_K = 30$ MeV, the charge density in the normal phase $Q_{\text{normal}} = 0.32 \text{ fm}^{-3}$, while in the CFL phase $Q_{\text{CFL}} = 0.09 \text{ fm}^{-3}$ (note that neutral CFL QM has $\mu_e = 0$ [17], so the charge density in CFL is due to the π^- density induced by μ_e). From the preceding arguments this implies that the volume fraction of the CFL phase in the mixed phase will be significantly larger. For the same reason, although the pairing contribution to the free energy itself is small, the equation of state of the CFL-nuclear mixed phase is considerably softer.

The equation of state for the CFL-nuclear and UQM-nuclear mixed phases are shown in Fig. 1. We see that if sharp transitions occur, then the occurrence of color superconductivity leads to higher energy density at low pressure because the NM→CFL transition ($a \rightarrow b$) occurs at lower pressure than NM→unpaired ($c \rightarrow d$), but lower energy density at high pressure, because CFL has a lower energy density than unpaired QM. On the other hand, if mixed phases occur, then color superconductivity leads to a higher energy density up to high pressures, since the NM+CFL mixed phase ($A \rightarrow B$) and CFL phase that follows it both have higher energy density than the NM+unpaired mixed phase ($C \rightarrow D$) over a wide range of pressures.

A mixed phase involving CFL and UQM is also allowed in principle. Such a mixed phase is characterized by a negatively-charged CFL phase coexisting with a

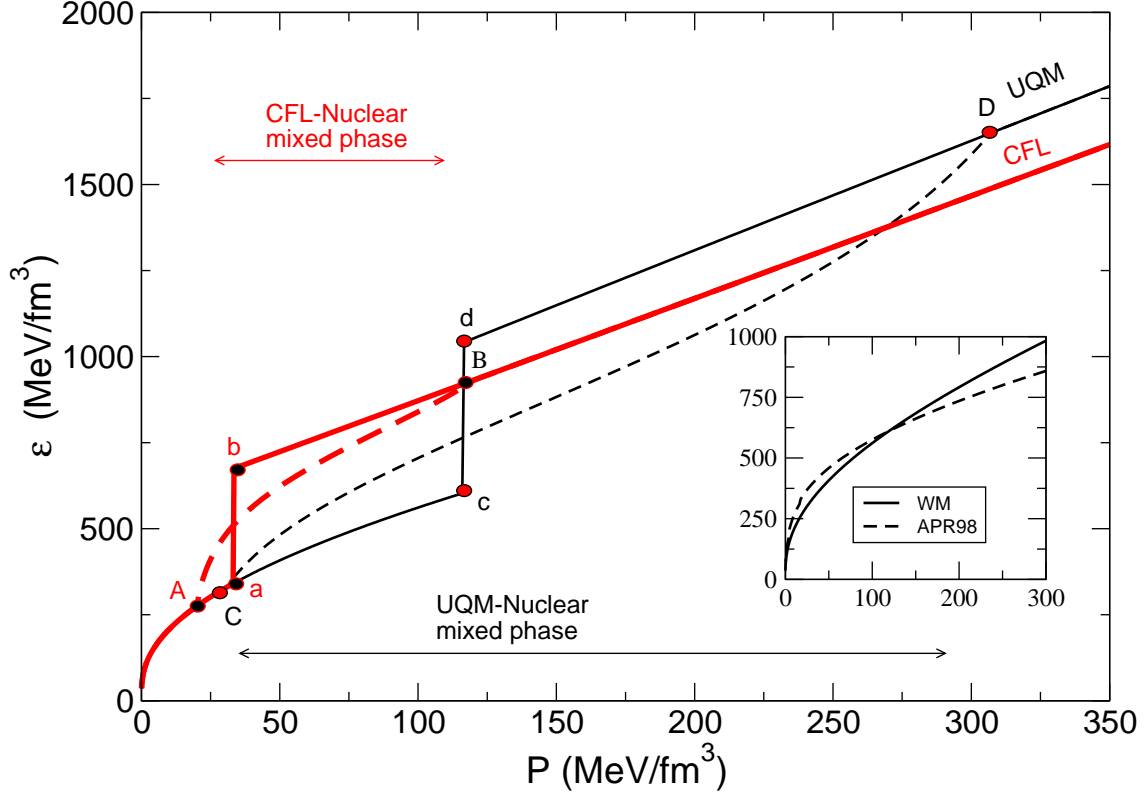


Figure 1: The equation of state for Walecka nuclear matter and quark matter with $B^{1/4} = 185$ MeV ($B = 153$ MeV/fm³) and $m_s = 200$ MeV. We show normal unpaired quark matter (thin lines) and color flavor locked superconducting quark matter with $\Delta = 100$ MeV (thick lines). We show neutral phases with sharp transitions (solid curves) and mixed phases (dashed curves). Differences between the Walecka model equation of state and the APR98 equation of state can be inferred from the figure inset.

positively-charged UQM phase. We find that such a mixed phase has lower free energy (even in the absence of surface and Coulomb effects) only if the negatively charged mesons (kaons) condense in the CFL phase. This requires that $\mu_e \geq m_K$. On the other hand, the UQM phase is positively charged only when $\mu_e \leq m_s^2/4\mu$. Further, the difference in free energy between this phase and the pure CFL phase is only of order m_s^4 and it does not greatly affect the equation of state. For these reasons we do not consider such a mixed phase in our study of the structure of the compact star. Nonetheless, the existence of such a mixed phase might have important consequences for transport and cooling phenomena especially in pure quark stars.

3 Compact Star Structure

To determine the mass and radius of the compact object for a given value of the central pressure, we must solve the Tolman-Oppenheimer-Volkov (TOV) equations [23],

$$\begin{aligned} \frac{\partial p}{\partial r} &= -G \frac{(p(r) + \varepsilon(p(r)))(M(r) + 4\pi r^3 p(r))}{r(r - 2GM(r))}, \\ \frac{\partial M}{\partial r} &= 4\pi r^2 \varepsilon(p(r)) \end{aligned} \quad (3.1)$$

where $\varepsilon(p)$ is the equation of state, i.e. the energy density as a function of the pressure, and $M(r)$ is the total energy enclosed within radius r .

By varying the central pressure it is possible to obtain the mass radius relation predicted for a given model description of the matter equation of state. The focus of this section is to employ the equations of state described in the previous section and deduce the corresponding mass-radius relationship.

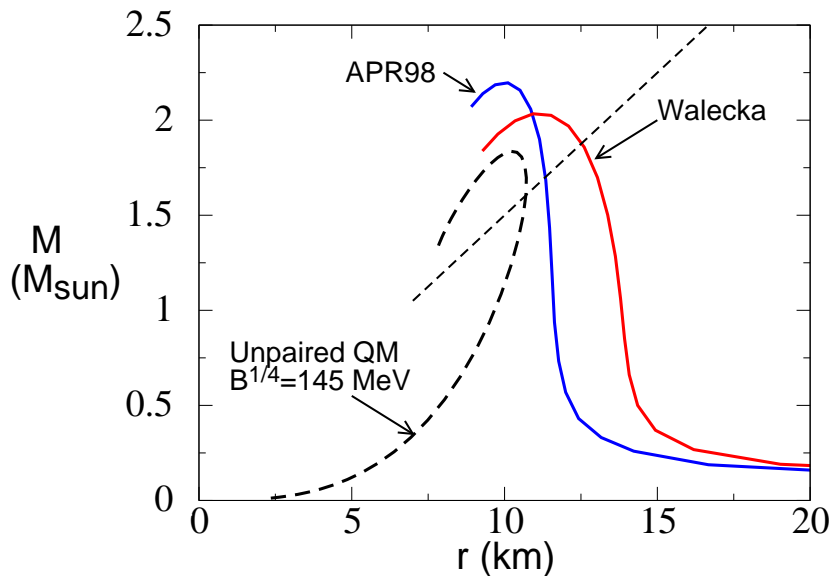


Figure 2: Mass-radius relationships for pure nuclear matter (NM) with Walecka and APR98 equations of state, and for unpaired quark matter with $B^{1/4} = 145$ MeV. The straight dashed line indicates the constraint obtained by recent measurements of the redshift of spectral lines from EXO0748-676 [24].

3.1 M - R relationship for uniform stars

First, we review the mass-radius relationship for the simple cases of stars made of pure nuclear matter or pure quark matter. The two solid curves in Fig. 2 are for pure nuclear matter stars. They follow from solving the TOV equation at high bag constant, so quark matter is highly disfavored and does not occur. There is one for each of the two nuclear equations of state that we use in this paper: the Walecka model (Section 2.1) and the APR98 tabulation [12]. They are roughly similar, showing the characteristic sharp rise in mass at $R \approx 10$ -15 km as the NM equation of state hardens around nuclear saturation density. They also show similar maximum masses of order $2 M_\odot$, at central densities of 5 to 10 times nuclear saturation density. Despite these similarities there are, as can be seen in the inset of Fig. 1, quantitative differences. The APR98 equation of state is on average softer at low density and stiffer at high density compared to the mean field model. For a detailed discussion of how different nuclear equations of state affect the mass-radius relationship of neutron stars see Ref. [25].

For comparison, Fig. 2 also shows (dashed line) the M - R curve for quark matter with no pairing ($\Delta = 0$) at a low bag constant ($B^{1/4} = 145$ MeV, $B = 58$ MeV/fm³) where three-flavor quark matter is favored over nuclear matter all the way down to zero pressure, but two-flavor quark matter is less favorable than nuclear matter at low pressure. The maximum mass is very sensitive to the bag constant, so the fact that this curve also shows a maximum at around $2 M_\odot$ is coincidental. (The mass and radius scale as $1/\sqrt{B}$ [15].) Not all the values of M and R that lie on the curves are stable. The family of stable configurations is generated by increasing the central pressure, and obtaining an increasing mass. As soon as the maximum of $M(p_{\text{central}})$ is attained, further increases in p_{central} , apparently yielding lighter stars, will in fact move onto the unstable branch. This means that the parts of the M - R curves to the left of the maxima in Figs. 2, 3 correspond to unstable stars.

3.2 M - R relationship for hybrid and color-superconducting stars

The main purpose of this paper is to explore the effect of quark pairing on the M - R relationship at values of the bag constant that are consistent with nuclear phenomenology. Fig. 3 shows the mass-radius curve for a plausible model of dense matter: the Walecka nuclear equation of state, and quark matter with physically reasonable values of the bag constant $B^{1/4} = 180$ MeV ($B = 137$ MeV/fm³) and strange quark mass $m_s = 200$ MeV [15]. Curves for unpaired ($\Delta = 0$) and color-superconducting ($\Delta = 100$ MeV) quark matter are shown. At these values the stars are typically “hybrid”, containing both quark matter and nuclear matter.

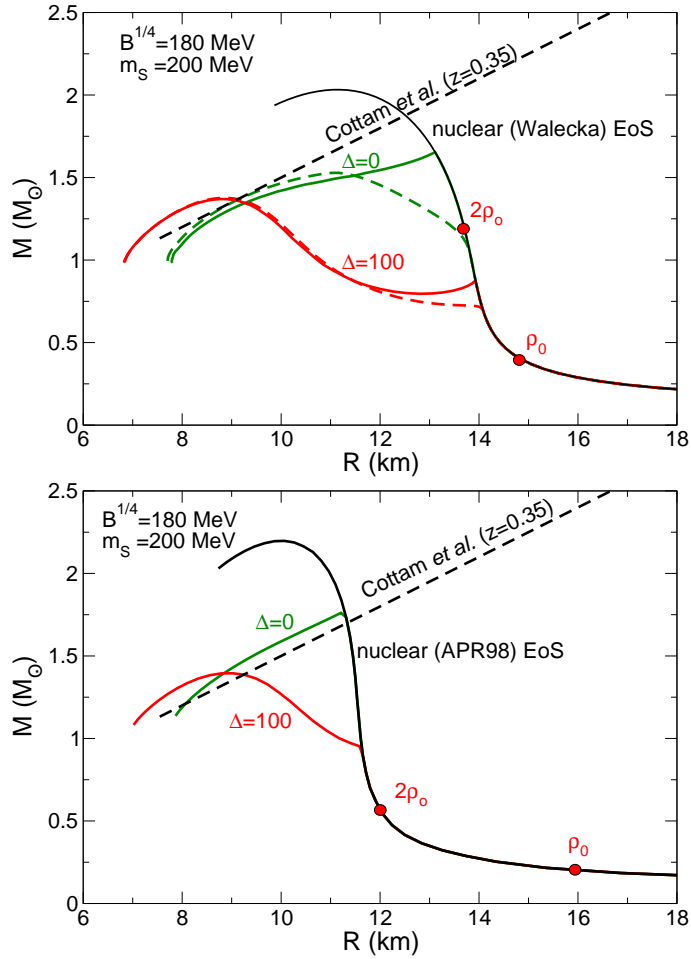


Figure 3: Mass-radius relationships at fixed bag constant $B^{1/4} = 180$ MeV and $m_s = 200$ MeV, for unpaired ($\Delta = 0$) and color-superconducting ($\Delta = 100$ MeV) quark matter. The mixed phase (dashed) and the sharp interface curves are shown. The line labeled “Cottam *et al.*” indicates the constraint obtained by recent measurements of the redshift on three spectral lines from EXO0748-676 [24]. The dots labeled ρ_o and $2\rho_o$ on the nuclear matter mass-radius curve indicate that the central density at these locations correspond to nuclear and twice nuclear saturation density respectively. The top panel uses the Walecka equation of state for nuclear matter, and the lower panel uses APR98 (in which case we only consider the sharp-interface scenario).

The solid lines in Fig. 3 correspond to stars that either have no QM at all, or a sharp transition between NM and QM: the core is made of quark matter, which is the favored phase at high pressure, and at some radius there is a transition to nuclear matter, which is favored at low pressure. The transition pressure is sensitive to Δ , for reasons discussed earlier. The dashed lines are for stars that contain a mixed NM-QM phase. In all cases we see that light, large stars consist entirely of nuclear matter. When the star becomes heavy enough, the central pressure rises to a level where QM, either in a mixed phase or in its pure form, occurs in the core. As can be seen from the figure the transition density is very sensitive to Δ .

The profiles of the maximum mass superconducting stars for different values of the bag constant, $\Delta = 100$ MeV and $m_s = 200$ MeV are shown in Fig. 4. For $B^{1/4} = 185$ MeV results for the sharp interface (denoted as (s)) and the mixed phase (denoted as (m)) scenario are shown. Here the maximum masses correspond to $1.33 M_\odot$ and $1.35 M_\odot$, respectively. The maximum mass for $B^{1/4} = 175$ MeV and $B^{1/4} = 170$ MeV are $M_{\max} = 1.44 M_\odot$ and $M_{\max} = 1.52 M_\odot$, respectively. This figure shows that the typical density discontinuity in the sharp interface scenario is $\approx 3\rho_0$. It also shows that for smaller values of B , the phase transition occurs very close to the surface of the star (at lower density as discussed earlier). The denser exterior regions of these stars (despite a less dense inner core) are primarily responsible for the increase in the maximum mass observed as one decreases B .

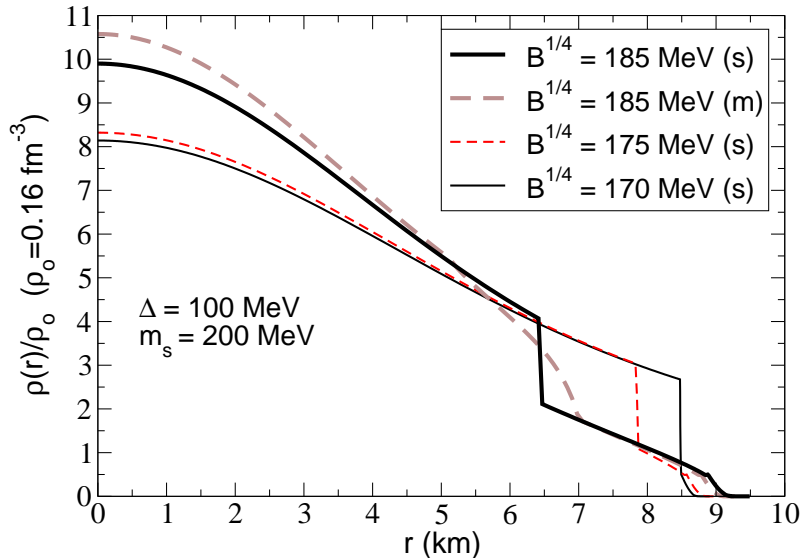


Figure 4: Profile of the maximum mass star for bag constant $B^{1/4} = 185, 175, 170$ MeV with $m_s = 200$ MeV and $\Delta = 100$ MeV. The mixed phase (dashed) and the sharp interface curves are shown. The Walecka model was used to describe the nuclear part of the EoS.

Fig. 4 indicates that in the mixed phase scenario there are no discontinuities in

the density profile of the star. However, this is not true in general. It is interesting to note that even when mixed phases are allowed, there can still be discontinuities in energy density within them. In a small range of parameters, we find stars that have a crust of nuclear matter surrounding a mixed NM-QM core, but the mixed phase has an outer part which is a mixture of unpaired QM with NM, and an inner part that is a mixture of CFL QM with NM. At the interface between the two there is a density discontinuity *within* the mixed phase¹.

The results shown in Figs. 3,4 indicate several generic trends:

1. The stability of stars containing pure QM but a without a QM-NM mixed phase (sharp-interface scenario) depends on the transition density. Color superconductivity helps the stability of these objects since it lowers the transition density and stiffens the equation of state relative to UQM.
2. In general, mixed phase stars are more likely to be stable since the adiabatic index changes smoothly in this case. For example, at $\Delta = 0$ the uniform phase stars become unstable as soon as quark matter is introduced (the $\Delta = 0$ line slopes down to the left, showing a decreasing mass as the central pressure rises) whereas the mixed phase (dashed line) gives a stable branch leading to a maximum mass $M_{\max} \approx 1.5 M_{\odot}$.
3. For large Δ there is very little difference between the sharp interface and mixed phase mass-radius curves. This is because the volume fraction of the CFL grows very rapidly within the nuclear-CFL mixed phase as discussed earlier in section 2.5. Consequently, the extent of the mixed phase is reduced and the EoS with in this region more closely resembles the pure CFL EoS as is evident from Fig. 1
4. Although there are visible differences between the mass-radius curves of the stars with UQM or CFL matter depending on whether one employs the Walecka or the APR98 equation of state, the maximum mass and corresponding radius of such a star is fairly independent of the nuclear equation of state. This is because the nuclear phase contributes very little to the total mass of these stars. These features of the mass-radius relation will be more comprehensively studied in section 3.3.
5. If the transition to superconducting quark matter is constrained to occur at or above nuclear density the maximum mass of these stars is $\approx 1.4 M_{\odot}$. It is possible to obtain larger masses ($\approx 1.6 M_{\odot}$) if the transition is allowed to occur at lower density. We elaborate further on this in the subsequent section.

3.3 Color superconductivity and the maximum mass

In bag model treatments of quark matter, the bag constant, strange quark mass, and the color superconducting gap are unknown parameters. In this paper we

¹The inclusion of additional phases, such as the 2SC phase, might modify this conclusion.

take a reasonable range of values for B and m_s , and study the dependence on Δ of observable features of compact stars such as their mass and radius. The resultant predictions can then be used to constrain the CFL color superconducting gap. In Fig. 5 we show how the maximum star mass (obtained by varying the central pressure) depends on color superconducting gap Δ for two different bag constants and two different strange quark masses.

For each value of the bag constant and strange quark mass there are two or three curves of M_{\max} vs Δ . The solid curve is for stars with some quark matter, paired or unpaired in them. The prominent dot on the curve separates the pure quark stars (to the right, at higher gap) from the stars with a QM core and a NM crust or mantle (to the left, at lower gap). The dotted curve indicates the heaviest pure NM star. This depends on the gap because Δ affects the point in the M - R plot at which quark matter appears. For example, for the equations of state used in the top panel of Fig. 3, the maximum NM mass would be $0.8 M_\odot$, (radius 13.8 km), since that is where QM first appears, and the star ceases to be pure NM. For the Walecka model that we used, the maximum possible NM mass is about $2.04 M_\odot$. For the APR98 equation of state, the maximum possible NM mass is about $2.20 M_\odot$. In general, a large gap favors quark matter, causing the heaviest pure NM star to become lighter.

(1) **Large bag constant**, $B^{1/4} = 185$ MeV, $B = 153$ MeV/fm³

(Upper two panels in Fig. 5).

(a) Pure NM stars still occur, but their maximum mass drops as the gap grows (dotted lines in Fig. 5) as the unstable QM branch cuts off the NM branch.

(b) Stars with a QM core and NM surface separated by a sharp interface (solid lines to the left of dots) become stable at gap $\Delta \sim 50$ -120 MeV, depending on m_s . These stars have mass $M \lesssim 1.5 M_\odot$.

(c) Stars with a NM-QM mixed phase core and NM surface (dashed lines) occur at lower values of the gap, and masses up to around $1.7 M_\odot$ are possible if the strange quark is heavy enough.

(d) Pure QM stars (solid lines to the right of dots) occur at very large gaps.

(2) **Small bag constant**, $B^{1/4} = 165$ MeV, $B = 96$ MeV/fm³

(Lower two panels in Fig. 5).

(a) Pure NM stars are again cut off by the QM branch.

(b) Stars with a QM core and NM surface separated by a sharp interface (solid lines to the left of dots) have masses up to about $1.6 M_\odot$. For light strange quarks $m_s \approx 150$ MeV, color superconductivity increases the maximum mass attained by the stars, but from a lower starting point at $\Delta = 0$.

(c) Stars with a NM-QM mixed phase core and NM surface (dashed lines) also have masses up to around $1.6 M_\odot$ if the strange quark is heavy enough.

(d) All QM-containing stars with mass greater than about $1.6 M_\odot$ are pure quark stars (solid lines to the right of dots).

The overall picture that emerges is that at these values of the bag constant, turning on color superconductivity does not raise the mass above about $1.8 M_\odot$.

We have not taken into account perturbative quantum corrections to the quark matter equation of state, but given the robustness of our conclusion with respect to variation in B , m_s , and Δ , it seems that a definitive observation of a star with mass over $2 M_\odot$ would be difficult to explain in terms of quark matter without invoking an even lower bag constant, with the danger that nuclear matter will be rendered unstable against two-flavor quark matter.

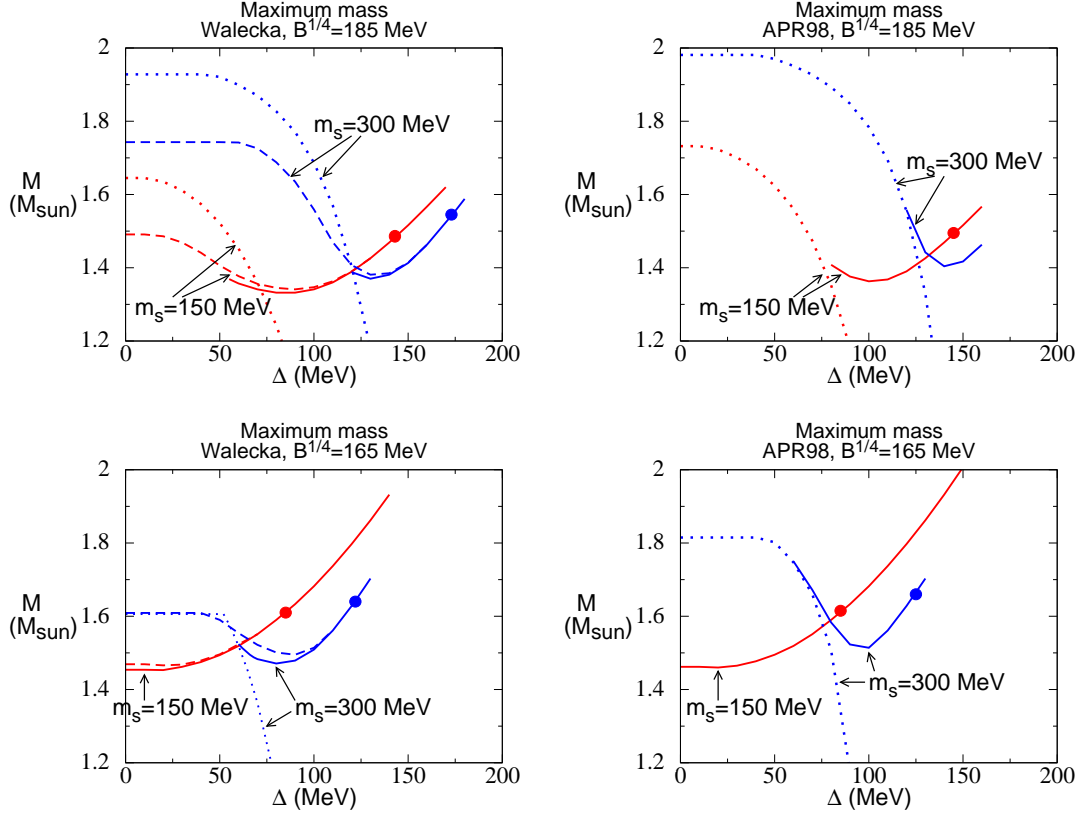


Figure 5: The maximum star mass (in solar masses) attained as a function of color superconducting gap Δ . The upper plots are for $B^{1/4} = 185$ MeV, the lower plots for $B^{1/4} = 165$ MeV. The left plots are for nuclear matter described by the Walecka model (in which case a mixed phase can be constructed). The right plots are for the APR98 nuclear equation of state for which we have only constructed locally neutral phases. Curves for strange quark mass $m_s = 150$ and 300 MeV are shown. The solid lines give the radius of stars with QM only (to the right of the dot), or a QM core surrounded by NM (to the left of the dot). The dotted lines show the heaviest pure NM star that occurs at the given gap Δ . The dashed lines are for stars that include a mixed phase.

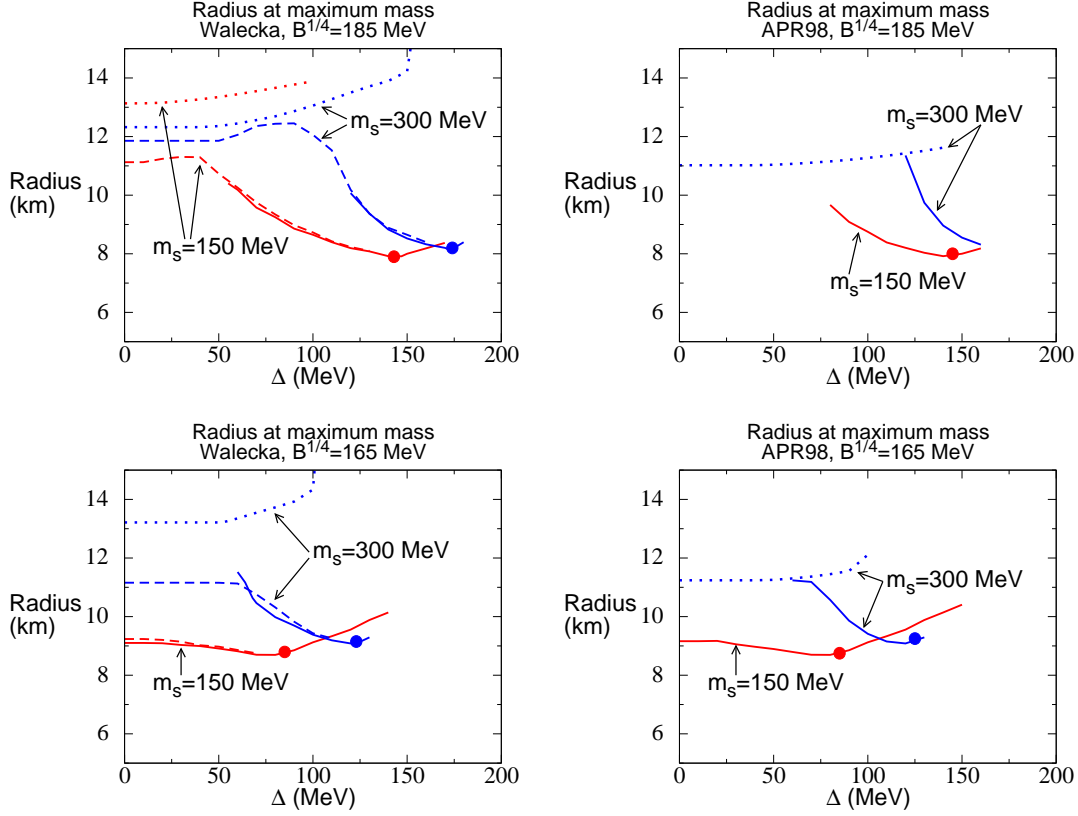


Figure 6: The radius of the star (in km) when it attains its maximum mass as plotted in Fig. 5. The upper plots are for $B^{1/4} = 185$ MeV, the lower plots for $B^{1/4} = 165$ MeV. The left plots are for nuclear matter described by the Walecka model (in which case a mixed phase can be constructed). The right plots are for the APR98 nuclear equation of state. Curves for strange quark mass $m_s = 150$ and 300 MeV are shown. The solid lines give the radius of stars with QM only (to the right of the dot), or a QM core surrounded by NM (to the left of the dot). The dotted lines show the heaviest pure NM star that occurs at the given gap Δ . The dashed lines are for stars that include a mixed phase.

3.4 Color superconductivity and compactness

By comparing the $\Delta = 100$ MeV curves of Fig. 3 with the UQM curve in Fig. 2, we see that superconductivity only has a moderate effect on the radius of the star. In Fig. 6 we investigate this issue more comprehensively, by plotting the radii of the stars whose masses appeared in Fig. 5, ie the radius of the heaviest star at each value of Δ for each equation of state. This confirms that color superconductivity does not affect the radii very strongly, but at low to medium gap $\Delta \lesssim 100$ MeV it tends to reduce them. This means that increasing Δ is *not* simply equivalent to decreasing the bag constant, in which case the mass and radius grow together as $1/\sqrt{B}$. By comparing Fig. 5 with Fig. 6 we see that when the maximum mass grows with Δ , the radius either decreases, or grows much more slowly. Overall, the stars that contain QM have radii between 8 and 12 km.

As one would expect from Fig. 3 the heaviest pure NM stars (dotted lines) have larger radii $\gtrsim 11$ km, since the QM stars replace the NM stars at low radius (high central pressure).

4 Conclusions

We have seen that color superconductivity has a considerable effect on the equation of state for quark matter. We can see from Eq. (2.14) and Fig.3 (see also Ref. [11]) that at values of the bag constant that would normally preclude compact stars from containing any QM, a large enough color-superconducting gap Δ can cancel out part of the bag constant, allowing a stable hybrid star to occur. In that sense, turning up Δ has a similar effect to turning down m_s or turning down B , but there are differences (see below).

The important question for the interpretation of future observations relates to the maximum mass of stars with quark matter in their core but a surface made of nuclear matter, as observed recently [24] (see detailed discussion below). Our overall conclusion is that in the range of bag constants and strange quark masses that we have studied, such stars have a maximum mass around $1.6 M_\odot$. This conclusion is based on our results presented in Fig. 5. The top panels show that color superconductivity allows QM-containing stars with a NM surface to occur at $B^{1/4} = 185$ MeV ($B = 153$ MeV/fm³), with masses up to about $1.5 M_\odot$. The lower panels show that at $B^{1/4} = 165$ MeV ($B = 96$ MeV/fm³) color superconductivity allows QM+NM stars to exist at high m_s , and at low m_s it boosts their mass: at $m_s = 150$ MeV a nuclear-surface star of mass $1.6 M_\odot$ is possible with $\Delta \sim 70$ MeV, whereas the maximum mass would be $1.45 M_\odot$ without color superconductivity.

It should be borne in mind that the QM+NM stars with masses near $1.6 M_\odot$ are dominantly quark stars with a thin NM crust (see Fig. 4). This is what one would expect, given that they occur just to the left of the dots on the curves on Fig. 5 which mark the point at which the star becomes pure QM. The NM→QM transition in such stars occurs at very low pressure ($\lesssim 1$ MeV/fm³) and at density

well below nuclear saturation density.

It is also interesting to note (see Fig. 6) that at low B and m_s color superconductivity increases the maximum mass without appreciably changing the radius. This is different from the effect of changing the bag constant, which increases the mass and radius together.

Finally, it is striking that even under the circumstances where color superconductivity has a noticeable effect on the maximum mass, it only does so for gap $\Delta \gtrsim 50$ MeV. Smaller gaps have little effect.

We emphasize that we have had no difficulty in constructing stars that are compatible with the recent results of Cottam, Paerels, and Mendez [24], who obtained a observational M - R curve by measuring the redshift of emission lines from highly ionized Oxygen and Iron in X-ray bursts from EXO0748-676. At radii of 8-12 km, their results suggest that the compact star mass is 1.2-1.8 M_\odot . Most of our stars fall in this range. Another constraint on the mass-radius of compact objects arise from recent observations of thermal radiation from RXJ185635-3754, an isolated neutron star. This combined with an accurate measurement of the distance to this object provide information about its radius. However, since the spectrum is not quite black body the inferred radius depends on theoretical models employed to describe the objects atmosphere [26, 27]. For this reason, the constraint from RXJ185635-3754 is weak and not as compelling as those derived from EXO0748-676. A simple black body fit yields radii that are small $R \sim 5$ km [28]. In our study here we were unable to construct stars with such small radii. Atmosphere models which best fit the observed data favor a large radius. In a recent article, Walter and Lattimer find that these model studies indicate that $R = 11.4 \pm 2$ km and $M = 1.7 \pm 0.4 M_\odot$ [27]. The superconducting quark stars constructed in this work are compatible with these results. These larger values for the mass and radius require a small bag constant, a large Δ and small m_s .

There are many ways in which this line of inquiry could be pursued further. (1) We treated the quarks as free, with a color superconducting gap at their Fermi surface. We did not include perturbative corrections to the equation of state [29], in other words, we set the strong coupling constant $\alpha_s = 0$. It would be useful to perform such calculations for CFL quark matter, and see how robust our conclusions are against variation in α_s . (2) We allowed two phases of quark matter, unpaired and CFL, and we did not include the two-flavor color superconducting “2SC” phase. Although this phase is generally unfavored [30, 31], it is just possible that there is a narrow range of m_s in which it can occur. Another competitor is the crystalline phase [32, 33]. It would be interesting to include these additional phases in our calculations. (3) We have used a general bag-model expression for the free energy of the quark matter, neglecting any possible density-dependence of the strange quark mass and color superconducting gap. We have also assumed that the bag constant takes the same value in all the quark matter phases, neglecting any differences of ground state energy between them. It would be interesting to use an NJL model to

calculate the quark matter equation of state, and thereby include these phenomena. One could also use a bag constant with a phenomenological density dependence [34].

It is very encouraging that observations of the radii of compact stars are becoming more precise. There have been significant developments in the theory of dense quark matter in the last few years, and we look forward to seeing whether the observed properties of compact stars are compatible with (or even require) the presence of the exotic phases of quark matter that are being so widely discussed.

Acknowledgments

We have had useful discussions with K. Rajagopal and V. Pandharipande. The research of MGA is supported in part by the UK PPARC. The research of SR is supported in part by funds provided by the U.S. Department of Energy (D.O.E.) under cooperative research agreement DF-FC02-94ER40818 and the D.O.E. contract W-7405-ENG-36.

References

- [1] B. C. Barrois, Nucl. Phys. B **129**, 390 (1977). S. Frautschi, Proceedings of workshop on hadronic matter at extreme density, Erice 1978. B. Barrois, “Nonperturbative effects in dense quark matter”, Cal Tech PhD thesis, UMI 79-04847-mc (1979).
- [2] D. Bailin and A. Love, Phys. Rept. **107**, 325 (1984).
- [3] M. Alford, K. Rajagopal and F. Wilczek, Phys. Lett. B **422**, 247 (1998) [hep-ph/9711395].
- [4] R. Rapp, T. Schäfer, E. V. Shuryak and M. Velkovsky, Phys. Rev. Lett. **81**, 53 (1998) [hep-ph/9711396].
- [5] M. Alford, K. Rajagopal and F. Wilczek, Nucl. Phys. B **537**, 443 (1999) [hep-ph/9804403].
- [6] M. G. Alford, Ann. Rev. Nucl. Part. Sci. **51** (2001) 131 [hep-ph/0102047]. K. Rajagopal and F. Wilczek, hep-ph/0011333. T. Schäfer and E. V. Shuryak, Lect. Notes Phys. **578** (2001) 203 [nucl-th/0010049]. D. K. Hong, Acta Phys. Polon. B **32** (2001) 1253 [hep-ph/0101025]. S. D. Hsu, hep-ph/0003140. D. H. Rischke and R. D. Pisarski, nucl-th/0004016.
- [7] M. G. Alford, hep-ph/0209287.
- [8] G. F. Burgio, M. Baldo, P. K. Sahu and H. J. Schulze, Phys. Rev. C **66**, 025802 (2002) [nucl-th/0206009].

- [9] K. Schertler, C. Greiner, J. Schaffner-Bielich and M. H. Thoma, Nucl. Phys. A **677**, 463 (2000) [astro-ph/0001467].
- [10] A. Steiner, M. Prakash and J. M. Lattimer, Phys. Lett. B **486**, 239 (2000) [nucl-th/0003066].
- [11] G. Lugones and J. E. Horvath, hep-ph/0211070.
- [12] A. Akmal, V.R. Pandharipande, D.G. Ravenhall, Phys.Rev. C **58** 1804 (1998) [nucl-th/9804027].
- [13] J. Negele and D. Vautherin, Nucl. Phys. **A207**, 298 (1973).
- [14] G. Baym, C. Pethick, D. Sutherland, Astrophys. J. **170**, 299 (1971).
- [15] N. K. Glendenning, *Compact Stars, Nuclear Physics, Particle Physics and General Relativity*, (Springer-Verlag, New York, 1997)
- [16] B. Serot and J. D. Walecka, *Advances in Nucl. Physics*, **16**, edited by J. W. Negele and E. Vogt (Plenum, New York, 1986)
- [17] K. Rajagopal and F. Wilczek, Phys. Rev. Lett. **86**, 3492 (2001) [hep-ph/0012039].
- [18] D. Son, M. Stephanov, Phys. Rev. D **61**, 074012 (2000) [hep-ph/9910491], erratum Phys. Rev. D **62**, 059902 (2000) [hep-ph/0004095].
- [19] P. F. Bedaque and T. Schäfer, Nucl. Phys. A **697** (2002) 802 [hep-ph/0105150].
- [20] D. B. Kaplan and S. Reddy, hep-ph/0107265.
- [21] N. K. Glendenning, Phys. Rev. D **46**, 1274 (1992).
- [22] M. G. Alford, K. Rajagopal, S. Reddy and F. Wilczek, hep-ph/0105009.
- [23] R. Tolman, Phys. Rev. **55**, 364 (1939); J. Oppenheimer and G. Volkoff, Phys. Rev. **55**, 374 (1939).
- [24] J. Cottam, F. Paerels, M. Mendez, Nature **420**, 51 (2002).
- [25] J. M. Lattimer and M. Prakash, Astrophys. J. **550**, 426 (2001) [astro-ph/0002232].
- [26] J. A. Pons, F. M. Walter, J. M. Lattimer, M. Prakash, R. Neuhauser and P. h. An, Astrophys. J. **564**, 981 (2002) [astro-ph/0107404].
- [27] F. M. Walter and J. Lattimer, Astrophys. J. **576**, L145-L148 (2002) [astro-ph/0204199].

- [28] J. J. Drake *et al.*, *Astrophys. J.* **572**, 996 (2002) [astro-ph/0204159].
- [29] E. Farhi and R. L. Jaffe, *Phys. Rev. D* **30**, 2379 (1984). B. A. Freedman and L. D. McLerran, *Phys. Rev. D* **16**, 1130 (1977); *Phys. Rev. D* **16**, 1147 (1977); *Phys. Rev. D* **16**, 1169 (1977); *Phys. Rev. D* **17**, 1109 (1978). V. Baluni, *Phys. Rev. D* **17**, 2092 (1978).
- [30] M. Alford and K. Rajagopal, *JHEP* **0206** (2002) 031 [hep-ph/0204001].
- [31] A. W. Steiner, S. Reddy and M. Prakash, hep-ph/0205201.
- [32] M. Alford, J. Bowers and K. Rajagopal, *Phys. Rev. D* **63**, 074016 (2001) [hep-ph/0008208].
- [33] J. A. Bowers and K. Rajagopal, hep-ph/0204079.
- [34] G. F. Burgio, M. Baldo, P. K. Sahu, A. B. Santra and H. J. Schulze, *Phys. Lett. B* **526**, 19 (2002) [astro-ph/0111440].